REVIEW

Check for updates

A review of anion-regulated multi-anion transition metal compounds for oxygen evolution electrocatalysis

Hao-Fan Wang, [iD] Cheng Tang, [iD] Bo-Quan Li and Qiang Zhang [iD] *

The oxygen evolution reaction (OER) is a research focus in the clean energy field because it is the core reaction in electrochemical water splitting, rechargeable metal–air batteries, *etc*. OER is a complicated four-electron process; thus, it suffers from slow reaction rates. Therefore, the exploration of efficient OER electrocatalysts has become a significant topic in the research of advanced energy materials. Transition metal compounds exhibit great potential as highly active OER electrocatalysts, and rational regulations have been applied to boost their OER performance. Among these strategies, anion regulation is an emerging but effective method to improve the OER activity of transition metal compounds. In this review, recent advances in anion-regulated multi-anion transition metal compounds as OER catalysts are introduced, including the synthesis methods, the regulation of anions and their effects on OER activity. Anion regulation during OER tests, *i.e.* surface oxidation of the catalysts, is also discussed in this review. Then, studies are introduced according to the type of regulated anion. This review is expected to provide further insight into the composition and structure regulation of OER catalysts and inspire further research into transition metal-based energy materials.

1. Introduction

The demand for sustainable energy sources and efficient energy devices is increasing rapidly. Therefore, new energy processes and advanced energy materials have recently become active topics of research.[1] Electrocatalysis of the oxygen evolution reaction (OER) is one of the most important of these processes and is attracting much attention. The OER plays a critical role in the fields of water splitting, metal–air batteries, *etc*.[2,3] Electrocatalytic water splitting is a promising method of hydrogen production, where the hydrogen evolution reaction (HER) occurs on the cathode and the OER occurs on the anode.[4] Metal–air batteries are regarded as the next generation of energy storage technologies; they have extremely high theoretical energy densities.[5–7] In metal–air batteries, OER takes place on the air electrode during the charge process. As

Beijing Key Laboratory of Green Chemical Reaction Engineering and Technology, Department of Chemical Engineering, Tsinghua University, Beijing 100084, China. E-mail: zhang-qiang@mails.tsinghua.edu.cn
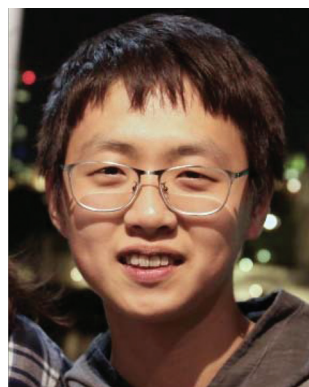
Hao-Fan Wang received his bachelor's degree from Tsinghua University in 2013. Currently, he is a Ph.D. candidate at Tsinghua University. His research focuses on advanced energy materials for applications in electrocatalysis, metal–air batteries, etc.
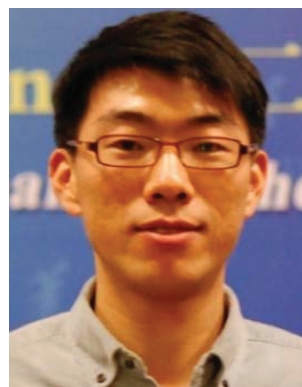
Hao-Fan Wang

Cheng Tang received his B.E. degree in 2013 in the Department of Chemical Engineering, Tsinghua University, where he is currently pursuing his Ph.D. His research interests focus on nanomaterials and energy electrocatalysis, including 3D graphene, hierarchical hybrids, oxygen reduction/evolution, and the hydrogen evolution reaction.

Cheng Tang

This journal is © the Partner Organisations 2018

Inorg. Chem. Front., 2018, **5**, 521–534 | 521

OER ($4OH^- \rightarrow O_2 + 2H_2O + 4e^-$ in alkaline electrolyte) is a four-electron reaction with complex reaction pathways and always exhibits high overpotential, it is considered to be a bottleneck of these related processes and devices.[8,9] Therefore, it is of great significance to explore efficient catalysts for OER.

Precious metal Ir- and Ru-based materials are acknowledged as state-of-the-art catalysts for OER; however, their applications are strongly limited by their scarce resources and high cost.[10,11] Transition metal (Mn, Fe, Co, Ni, *etc.*) compounds and carbon nanomaterials have been widely investigated as alternatives to precious metal catalysts.[9,12–28] The OER activity of an electrocatalyst depends on the mass transport from the electrolyte to the catalyst surface, the electrical conductivity of the catalytic material, and the intrinsic activity of the active sites.[29,30] Meanwhile, the intrinsic activity is affected by the interactions between the active sites and the adsorbed oxygen-containing species. An OER process involves the adsorption of OH^- (alkaline media) or H_2O (acid media), the formation of oxygen–oxygen bonds, the desorption of O_2, *etc.* The activity of each step is related to the adsorption energy of the oxygen-containing species on the active sites. The relationship between the OER activity and the adsorption energy can be described by a volcano plot.[29,31] At a specific adsorption energy, the active sites can achieve the best performance. Adsorption energy that is either too high or too low can lead to decreased OER reactivity. Therefore, the activity of the active sites can be optimized by tuning the adjacent atoms. The adjacent atoms can regulate the electronic structures of the active sites, thus influencing their interactions with oxygen-containing species.

For transition metal compounds, the transition metal atoms, such as Fe, Co, and Ni, are regarded as the active sites to adsorb oxygen-containing species. The electronic structures of these active sites can be coordinated by doping, etching, and substitution of ions.[32] According to the type of ion being regulated, these activity regulation methods can be classified as cation regulation or anion regulation. The cation regulation method has been more widely investigated due to the increas-

ing research on the electrocatalysis of OER in the past decade. For example, doping of Fe in Ni and Co (oxy)hydroxides can regulate the chemical state and the atomic arrangement of Ni/Co, thus enhancing their OER activity.[33–36] To date, Fe/Co/Ni-based composites have become an important group of alternatives to precious metal OER catalysts.[9,12,13,24,37–52] Other representative studies on cation-regulated OER catalysts include the etching of p-block metal ions in perovskite catalysts to provide abundant surface defects,[53] the modulation of the Ni redox properties in NiFe oxides by incorporating redox-inert Al^{3+} ions,[54] the doping of W^{6+} in FeCo oxyhydroxides,[55,56] and the integration of Cu^+ and Cu^{2+} in copper oxides.[57] In addition to cation regulation, anion regulation on electrocatalysts has been gradually attracting increasing attention in recent years.[58,59] Similar to cation regulation, through the doping, etching, and substitution of anions, the interactions between the active sites and adjacent atoms and the atomic arrangements around the active sites can be modulated. Moreover, as the ionic radii of anions are much larger than those of metal ions, anion regulation can bring about greater changes in the structures of catalysts.[60]

There have been several reviews on transition metal-based OER catalysts based on various anions, such as oxides,[14] hydroxides,[61] sulfides,[15,37,62,63] nitrides,[64] and phosphides.[37,65,66] However, no specific review on the anion regulation of OER catalysts has been published. In this review, we will focus on anion regulation on transition metal compound OER catalysts with multiple anions. These materials usually contain external anions incorporated into the lattices of metal compounds. This incorporation can lead to a relatively disordered structure with a larger surface area and lower steric hindrance for the adsorption and desorption of oxygen-containing species. The anion-regulated OER electrocatalysts are introduced according to the type of anions contained in the inorganic materials. As a special case, oxygen incorporation during OER tests is also discussed. The primary focus will be on the effects of anion regulation on OER activity. We hope
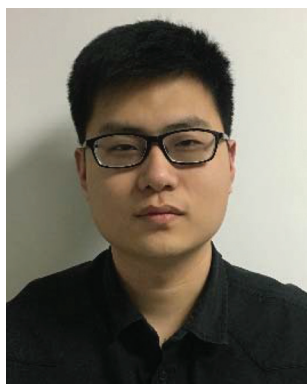
Bo-Quan Li received his B.S. degree in 2016 in the Department of Chemistry, Tsinghua University, and is currently a Ph.D. student in the Department of Chemical Engineering. His research interests focus on advanced materials for electrochemical energy storage.

Bo-Quan Li

Qiang Zhang received his bachelor's and Ph.D. degrees from Tsinghua University in 2004 and 2009, respectively. After stays at Case Western Reserve University, U.S.A., and the Fritz Haber Institute of the Max Planck Society, Germany, Prof. Zhang joined Tsinghua University in 2011. He held the Newton Advanced Fellowship from the Royal Society, U.K. and was a NSFC Young Scholar in China. His current research interests are advanced energy materials, including lithium metal anodes, lithium sulfur batteries, and electrocatalysis.

Qiang Zhang

This journal is © the Partner Organisations 2018

this review will provide stimulatory knowledge for developing OER electrocatalysts and inspire more insights into anion regulation on transition metal compounds, leading to high-efficiency designs and synthetic strategies for advanced energy storage and conversion materials.

2. Anion regulation during OER tests

Although catalysts can theoretically remain unchanged before or after a reaction, the evolution of electrocatalysts is observed on many practical occasions. OER is performed at oxidizing potentials; thus, the surface of the catalysts can be oxidized during the reaction process. In common alkaline electrolytes for transition metal-based catalysts, O^{2-} or OH^- can replace the original anions in the catalyst. Jin[67] pointed out that this process is responsible for the OER activity of chalcogenides, nitrides, and phosphides. This phenomenon indicates that most metal-based OER catalysts are actually anion-regulated when catalyzing the reaction, and the anion regulation method is effective in enhancing the OER activity.

A typical example of anion regulation during OER tests is the transformation of Co_3O_4 catalysts. Co_3O_4 has been widely investigated for efficient OER catalysis,[68–73] and its surface oxidation during the OER process has also been reported.[74–77] With the oxidation of cobalt ions, the OH^- ions in the electrolyte are doped in Co_3O_4, forming a $CoOOH$ or $CoO_x(OH)_y$ structure. Strasser and co-workers proposed *in situ* structural characterizations on Co_3O_4 at different OER potentials.[74] The OER tests were carried out in 0.10 M KP_i at pH 7. Fig. 1a shows the cyclic voltammogram (CV) plot of the Co_3O_4 catalyst; the onset potential is about 1.6 V *vs.* a reversible hydrogen electrode (RHE). In the following structural characterizations, the

Co_3O_4 samples were analyzed before OER tests (*ex situ*), at the testing potentials of 1.00, 1.22, 1.55, and 1.62 V, and after OER tests. 1.62 V was the OER active potential. A summary of the results of the X-ray absorption measurements, including X-ray absorption near edge structure (XANES) and extended X-ray absorption fine structure (EXAFS) studies, is presented in Fig. 1b. The upper portion of Fig. 1b shows the shift of the Co X-ray adsorption K-edge; the positive shift represents a higher oxidation state. This indicates that the Co ions are gradually oxidized as the potential increases. The local atomic structure of Co ions can be assessed by EXAFS simulations. Co_3O_4 contains two types of cobalt ions: one Co^{2+} ion in the tetrahedral site and two additional Co^{3+} ions in the octahedral site. The lower part of Fig. 1b exhibits the quantity variation of cobalt ions with these two configurations by EXAFS analyzes. Mono-μ-oxo represents the tetrahedral site and di-μ-oxo represents the octahedral site. A shift towards more di-μ-oxo-bridged, octahedrally coordinated Co ions in the OER-active state (1.62 V) was observed, confirming the oxidation of Co ions. Thus, the surface of the cobalt oxide catalysts is believed to convert to cobalt oxyhydroxide at OER potentials, exhibiting an amorphous structure, as shown in Fig. 1c. This anion regulation process in alkaline electrolyte was also reported by Liu *et al.* and Friebel *et al.*[76,77] Moreover, Bell and co-workers reported theoretical investigations of the activity of cobalt oxides for the electrochemical oxidation of water; they identified β-CoOOH as the active phase.[75] In short, at OER potentials, the surface of the Co_3O_4 catalyst is anion-regulated to an activated oxyhydroxide phase with the co-existence of O^{2-} and OH^-, showing superior reactivity. Because of their high OER activity, oxyhydroxides have been widely investigated and are currently the most reported multi-anion transition metal compounds for OER electrocatalysis.[33,34,78–83]
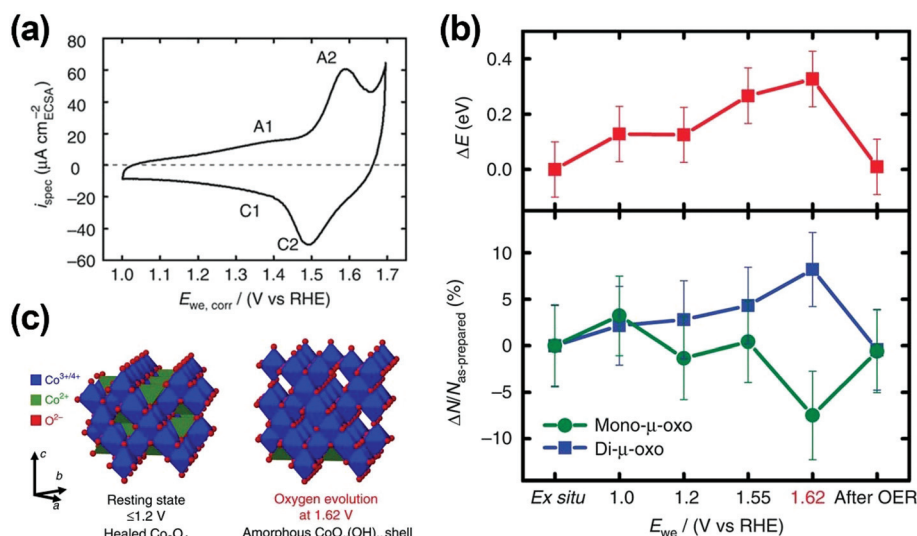

Fig. 1 Anion regulation during the OER process of Co_3O_4. (a) Cyclic voltammogram of Co_3O_4 catalyst in 0.10 M KP_i at pH 7. (b) Shift of the Co X-ray absorption K-edge (upper); changes in the EXAFS coordination numbers of the di- and mono-μ-oxo bridges between Co ions (lower) with respect to the as-prepared (*ex situ*) state. The state at 1.62 V corresponds to the catalytically active oxygen evolution state. (c) The crystal structure of Co_3O_4 (left) and a possible crystal structure at OER active potential (right).[74] Copyright 2015 Nature Publishing Group.

This journal is © the Partner Organisations 2018

Inorg. Chem. Front., 2018, **5**, 521–534 | **523**

Studies on transition metal chalcogenides, nitrides, and phosphides are not as numerous as studies on oxides; however, their surface transformations during the OER process have also been reported in several publications.[84–89] When oxygen is incorporated, the surface atomic configuration is modulated, and this anion-regulated layer usually exhibits an amorphous structure. The active phases of these catalysts are the anion-regulated multi-anion materials generated at OER potentials. Anion regulation always occurs during the OER process in transition metal-based catalysts. However, the anion regulation during OER was rarely discussed and elucidated. Therefore, the selected examples that are discussed in the following sections only involve energy materials with designed anion regulation during the synthesis process. Anion/cation regulation of metal compounds can also take place in applications other than OER, such as metal ion batteries.[90] It is promising to propose new methods of ion regulation based on these applications.

3. Designed anion-regulated transition metal compounds for OER

3.1 Transition metal compounds with O^{2-}/OH^-

Compared with other transition metal compounds, both oxides and hydroxides are more readily synthesized because the oxygen atoms can be easily obtained from air and water. Therefore, many reported multi-anion OER catalysts contain oxygen. In this section, these catalysts will be introduced in terms of the types of anions that are incorporated with O^{2-} or OH^-.

3.1.1 Oxygen and other chalcogens. The chalcogens are the chemical elements in group 16 of the periodic table. This group includes the elements O, S, Se, Te, etc. Transition metal chalcogenides (TMCs), especially sulfides and selenides, have recently received tremendous attention in oxygen electrocatalysis.[37,91–101] The catalytic activity of TMCs can be further increased by oxygen incorporation.

Recently, Zhang's group reported anionic-regulated NiFe oxysulfides as OER electrocatalysts.[32] Firstly, they proposed a mechanism of anion regulation, as shown in Fig. 2a. The ionic radius of O^{2-} is smaller than that of S^{2-}. Therefore, O^{2-} displays lower polarizability, and S^{2-} shows higher polarizability. In Fig. 2a, M^+ represents the metal cation, which serves as the active site. X^- is the anion with lower polarizability (O^{2-} in this work), and Y^- is the anion with higher polarizability (S^{2-} in this work). In compound MX (left), the X^- ions appear to have dominant ionicity and the electron interaction is weak. M^+ ions can provide a strong positive electric field, which is favorable for hydroxyl adsorption but detrimental to the desorption of oxygen. In contrast, for compound MY (right), the Y^- ions are dominantly polarized, and the electrons can fill the empty orbits of the M^+ ions. Therefore, the adsorption of negative hydroxyls is obstructed. By regulating the ratio of X^- and Y^- in a compound, the electronic structure of its active sites can be optimized towards the highest reactivity (middle). Anion regu-

lation of the electrocatalysts was realized by sulfurization of a NiFe hydroxide precursor using thioacetamide (TAA) as the sulfurization reagent. The product was named NiFeS-x, where x marks the mass ratio of TAA : NiFe hydroxide; NiFeS-x exhibited the morphology of oxysulfide nanoparticles supported on graphene sheets. Four samples, NiFeS-0, NiFeS-0.5, NiFeS-2, and NiFeS-8, were selected in the electrochemical tests; their S contents increased with the ratio of TAA used in the sulfurization process. The OER linear sweep voltammetry (LSV) plots of the four samples are presented in Fig. 2b. Fig. 2c illustrates the volcano plot of OER reactivity characterized by the overpotential at 10.0 mA cm^{-2} (η_{10}) against the sulfurization degree under anion regulation. NiFeS-2 exhibits the highest OER activity, with an η_{10} value of 286 mV. In the X-ray photoelectron spectroscopy (XPS) spectra (Fig. 2d), the Fe 2p and Ni 2p spectra exhibit downshifts with increasing S content. This result supports the anion regulation theory described in Fig. 2a. With an appropriate oxygen/sulfur ratio, the Fe and Ni active sites were regulated to optimized electronic structures, leading to superior OER activity.

Through anion regulation of sulfur and oxygen, Zhang's group further proposed a unique hydroxysulfide electrocatalyst for the first time.[102] Metal hydroxides were also utilized as the precursor, and the sulfurization was carried out by simply immersing the hydroxide precursor into a solution with a high concentration of S^{2-}. The S^{2-} continuously replaced the OH^- in the solid phase according to the solubility equilibrium. The S content in the hydrosulfide resultant could be easily regulated by tuning the S^{2-} concentration and the immersing time. Scanning electron microscopy (SEM) and transmission electron microscopy (TEM) images of the anion-regulated CoFe hydroxysulfide ($Co_3FeS_{1.5}(OH)_6$) loaded on a nitrogen-doped graphene material are shown in Fig. 3a and b, respectively. A control sample synthesized through a hydrothermal method using CoFe hydroxide and TAA was also obtained. This hydrothermal electrocatalyst had higher sulfur content and a larger particle size; it was denoted as $CoFeS_{1.6}(OH)_{1.8}$-HT (where HT refers to hydrothermal synthesis). In the OER tests in 0.10 M KOH, the room-temperature converted hydroxysulfide exhibited excellent OER activity that was comparable to that of an IrO_2 catalyst due to its appropriate amount of S-doping and its smaller particle size. The OER η_{10} was 358 mV according to the LSV plots (Fig. 3c), and the Tafel slope was calculated to be 79 mV dec^{-1} (Fig. 3d).

Anion regulation of S and O was also realized by substituting $Fe(CN)_6^{3-}$ with S^{2-} in metal Prussian Blue Analogue (PBA) compounds.[103] The amorphous $CoS_{4.6}O_{0.6}$ porous nanocubes prepared by this method afforded an OER η_{10} of 290 mV in 1.0 M KOH, which was better than that of RuO_2 (300 mV). This oxysulfide catalyst also exhibited superior OER activity to RuO_2 in neutral electrolyte. Calcination is an effective method to tune the sulfur and oxygen contents of oxysulfides. As reported by Zhang et al.,[104] oxygen atoms were incorporated in NiFe sulfides (NFS) after calcination at 200 °C in air. The obtained O-NFS could provide an OER current density of 200 mA cm^{-2} at an overpotential of 312 mV; meanwhile, this overpotential

524 | Inorg. Chem. Front., 2018, 5, 521–534

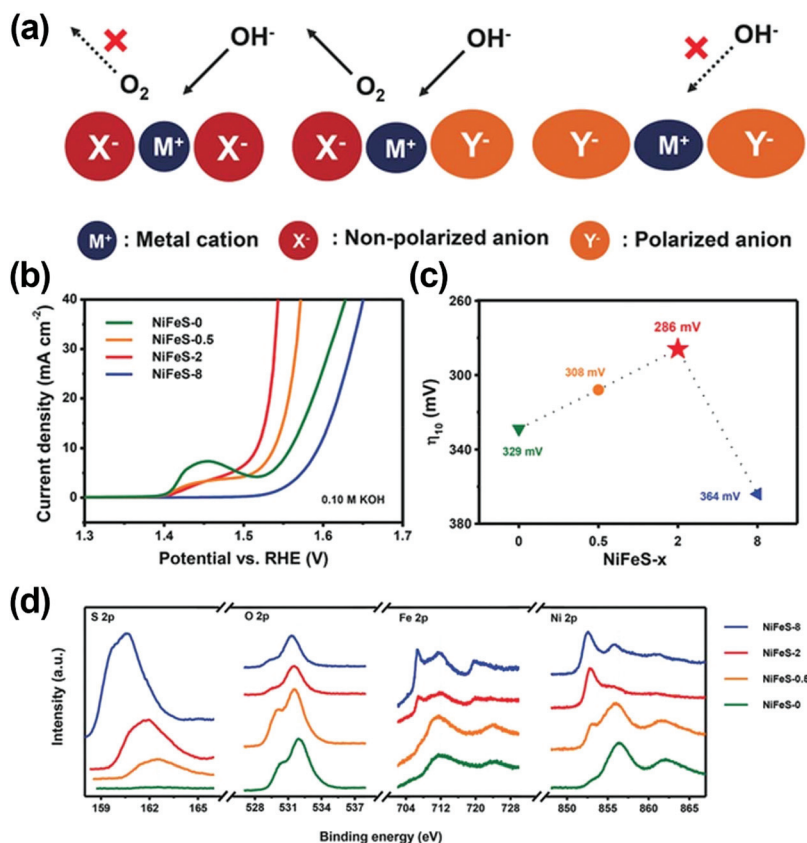This journal is © the Partner Organisations 2018

Fig. 2 Anion regulation of oxygen and sulfur in oxysulfides. (a) Schematic of the mechanism of anion regulation on transition metal compounds for OER electrocatalysis. (b) OER LSV plots of oxysulfide materials with different S contents, tested at a scan rate of 10 mV s^{-1} in O$_2$-saturated 0.10 M KOH electrolyte. (c) A volcano-type plot of the overpotential required for 10 mA cm^{-2} OER current density vs. sulfurization degree. (d) High resolution S 2p, O 2p, Fe 2p, and Ni 2p XPS spectra of the oxysulfide materials. The anion-regulated electrocatalysts exhibited shifts to lower binding energies.[32] Copyright 2017 Wiley-VCH.

was 334 mV for NFS. It is worth noting that the high current densities reported in this work were partly attributed to the high catalyst loading amounts on the Ti plates. Chen and co-workers calcinated oxysulfides in an ammonia flow.[105] In the ammonia atmosphere, oxygen vacancies were generated in the oxysulfides by ammonolysis, and nitrogen atoms were doped into the graphene support. The resulting N-doped graphene-supported CoO$_{0.87}$S$_{0.13}$ showed a low OER η_{10} of 357 mV in 0.1 M KOH.

3.1.2 Oxygen and nitrogen. Oxynitrides are complex salts containing oxygen and nitrogen that are well known for their photochemical properties. The oxynitrides have been investigated as photocatalysts for water splitting, phosphors for white light-emitting diodes, etc.[106–114] Recently, a CoMn oxynitride (CoMnON) for oxygen electrocatalysis was reported by Fujita, Sasaki, and co-workers.[115] The oxynitride was synthesized through the nitriding of spinel-type CoMn oxide at high temperature under ammonia flow. CoMnON exhibited a NaCl-type structure, as shown by its X-ray diffraction (XRD) patterns (Fig. 4a). The composition of the resulting products was regulated by the calcination temperature. The N/O atom ratio of the CoMnON obtained at 550 °C was 1 : 0.13, measured by energy-dispersive X-ray spectroscopy (EDS). Fig. 4b and c show

the TEM images of 550 °C-annealed CoMnON. CoMnON nano-particles with an average size of 5 nm were observed. The OER LSV plots tested in O$_2$-saturated 0.10 M KOH are presented in Fig. 4d. The nitrogen-incorporated CoMnON exhibited larger OER current density than the undoped oxide CoMnO, with η_{10} values of 0.47 vs. 0.54 V on the CoMnON and CoMnO electrocatalysts, respectively. This nitriding method can be applied to other spinel compounds to enhance their OER activity.[115]

Compared with oxynitrides, transition metal nitrides have been more widely investigated as oxygen electrocatalysts.[64,116–121] Nanoscale mixtures of nitrides and oxides have also been reported as efficient electrocatalysts for OER, and the interfaces between nitrides and oxides play a prominent role in promoting their OER activity.[122,123] Therefore, it is promising to perform homogeneous nitrogen-doping in oxides, or oxygen-doping in nitrides, to achieve superior OER electrocatalysis.

3.1.3 Oxygen and phosphorus. Transition metal phosphides are also an important group of materials in electrochemistry.[88,124–132] The OER electrocatalytic activity of phosphides was first reported by Du's group and Hu's group simultaneously in 2015.[88,128] In some of the works using phosphides as OER electrocatalysts, irreversible surface oxidation
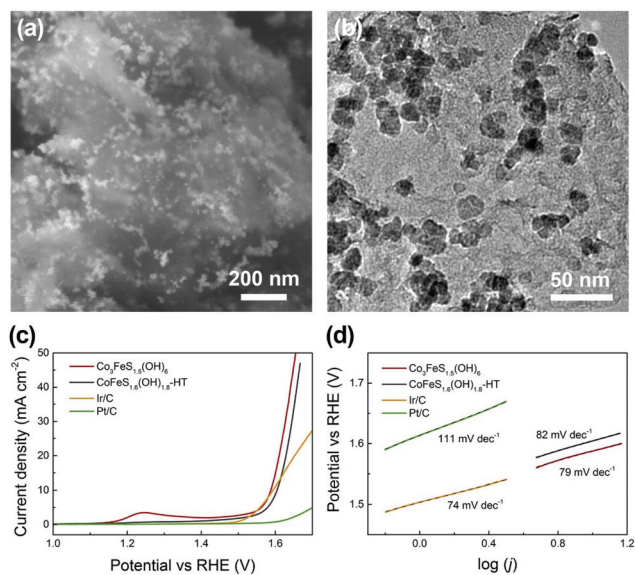
This journal is © the Partner Organisations 2018

Inorg. Chem. Front., 2018, 5, 521–534 | 525

Fig. 3 Anion regulation of oxygen and sulfur in hydroxysulfides. (a) SEM and (b) TEM images of anion-regulated hydroxysulfide $Co_3FeS_{1.5}(OH)_6$ supported on N-doped graphene. (c) OER LSV plots of room-temperature converted hydroxysulfides, hydrothermal synthesized hydroxysulfides, and commercial precious metal catalysts Ir/C and Pt/C, measured at a scan rate of 10 mV s^{-1} in O_2-saturated 0.10 M KOH electrolyte. (d) Tafel plots derived from the LSV plots.[102] Copyright 2017 Wiley-VCH.

was observed, and the OER activity increased after a period of reaction.[88,125,128] The incorporation of oxygen in phosphides enhances their OER activity. In this section, the anion regulation of O and P for efficient OER electrocatalysis will be introduced.

The concept of anion regulation (also called anion modulation) in electrocatalysis was firstly proposed by Qiao's group in 2016.[133] Anion regulation (O and P) and cation regulation (Co and Fe) were conducted simultaneously for overall water splitting. This Fe- and O-doped Co_2P catalyst, named CoFePO, was synthesized by the following method. Firstly, CoFe hydroxides were grown on nickel foam by a chemical bath deposition (CBD) method. Then, P anions were introduced by annealing CoFeOH in the presence of triphenylphosphine (TPP) in N_2 atmosphere. The regulation of P and O in CoFePO was realized by using different amounts of TPP in the annealing process. The main CoFePO sample was synthesized using 2.013 g TPP and CoFe hydroxides derived from 291 mg $Co(NO_3)_2\cdot6H_2O$ and 40.4 mg $Fe(NO_3)_3\cdot9H_2O$. The electron energy loss spectroscopy (EELS) mapping in Fig. 5a confirmed the coexistence of Co, Fe, P, and O in the catalyst. The XRD patterns (Fig. 5b) indicated that the structure of CoFePO was similar to that of Co_2P. The CoFePO catalyst was therefore identified as Fe- and O-doped Co_2P. To regulate the P/O ratio, different amounts of TPP were applied for phosphorization. According to the ratio of the TPP amount to the original amount (2.013 g), the anion-regulated CoFePO samples were named CoFePO-0.325, 0.75, 1, 1.25, and 1.5. The HER and OER LSV plots are shown in Fig. 5c and d, respectively. The η_{10} values of OER, HER and overall water
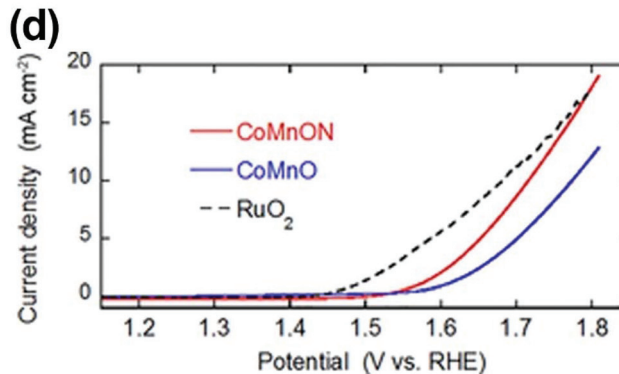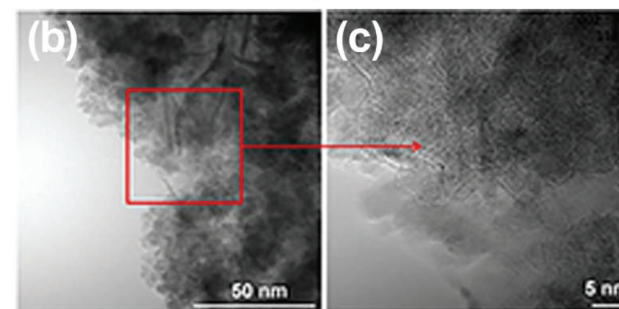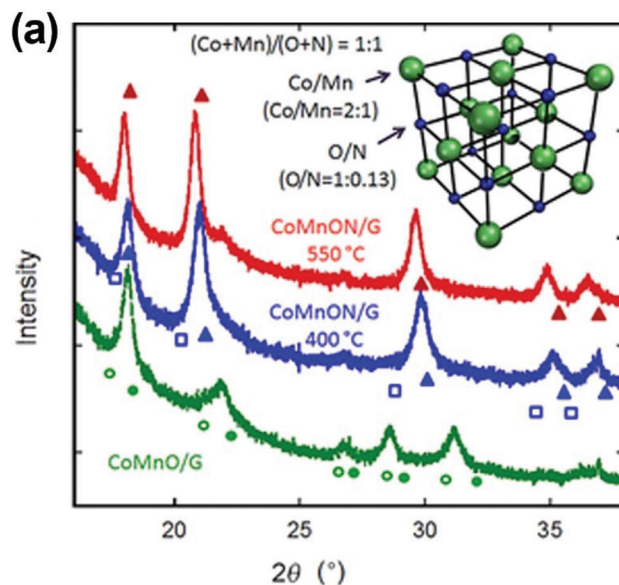

Fig. 4 Anion regulation of oxygen and nitrogen in oxynitrides. (a) XRD patterns of CoMn oxides and CoMn oxynitrides obtained at 400 °C and 550 °C. Inset: Schematic of the crystal structure of CoMnON (550 °C). (b) and (c) TEM images of CoMnON annealed at 550 °C. (d) OER LSV plots of CoMnON, CoMnO, and commercial RuO_2 tested in O_2-purged 0.10 M KOH solution at a scan rate of 10 mV s^{-1}.[115] Copyright 2017 Wiley-VCH.

splitting are summarized in Fig. 5e. With increasing P/O ratio, the catalytic activity presented a trend of early increase and later decrease. This trend can also be explained by the higher polarizability of P ions compared to O ions. Thus, the adsorption of the reactants was weakened and the desorption of the products was enhanced with increasing P content. As a result, the best OER activity was achieved on the electrocatalyst with a
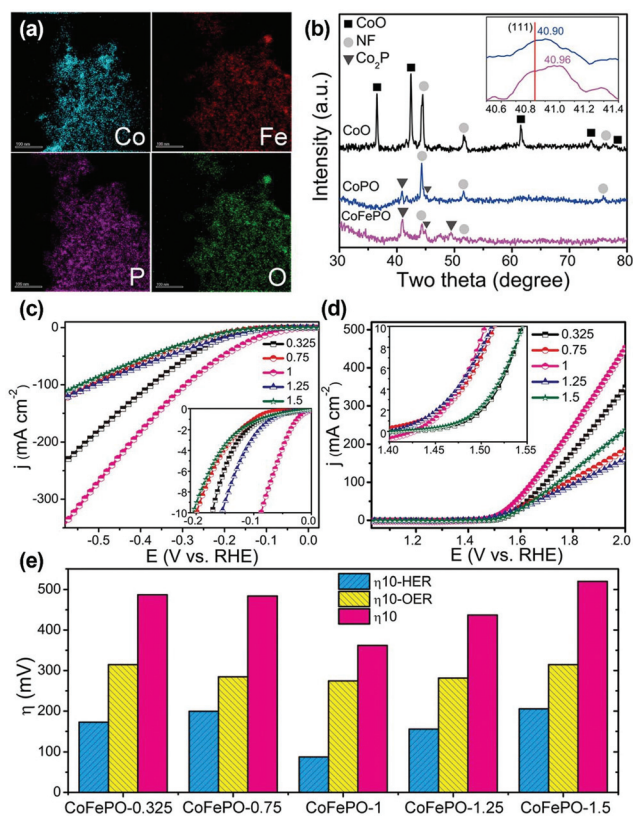
526 | Inorg. Chem. Front., 2018, 5, 521–534

This journal is © the Partner Organisations 2018

Fig. 5 Anion regulation of oxygen and phosphors in oxygen-doped metal phosphides. (a) TEM EELS mapping of Co, Fe, P, and O elements in CoFePO. (b) XRD patterns of CoO, CoPO, and CoFePO. The XRD patterns of the phosphatized materials are similar to that of Co_2P (JPCDS No. 54-0413). (c) HER and (d) OER LSV plots of CoFePO with different phosphorization degrees. All the testing was conducted in 1.0 M KOH electrolyte. (e) Summary of the overpotentials at a current density of 10 mA cm^{-2}.[133] Copyright 2016 American Chemical Society.

medium P/O ratio. The CoFePO-1 sample with a P/O ratio of 0.42 exhibited the best OER performance, with a η_{10} of 274.5 mV. Similarly, the annealing of nickel hydroxides in the presence of a P source was performed by Wu et al.[134] Oxygen-incorporated Ni_2P was obtained via this method and showed significantly increased OER activity compared with $Ni(OH)_2$ and Ni_2P.

Recently, Wang and co-workers reported a P-doped Co_3O_4 material as a water splitting electrocatalyst; the material maintained the Co_3O_4 spinel structure after P doping.[135] Under Ar plasma etching, oxygen vacancies were generated in Co_3O_4, forming V_O-Co_3O_4. In the presence of a P source (NaH_2PO_2 in this work), P atoms could fill the oxygen vacancies; the resulting product was named P-Co_3O_4. Fig. 6a shows a TEM image of P-Co_3O_4. The lattice fringes of spinel Co_3O_4 can be clearly observed in the high-resolution TEM (HRTEM) image of the framed area (Fig. 6b). The EDS mappings confirmed the uniform filling of P atoms in Co_3O_4 (Fig. 6c). The OER LSV plots and Tafel plots measured in 1.0 M KOH are shown in Fig. 6d and e, respectively. The OER activity of Co_3O_4 improved after the formation of oxygen vacancies, and the activity was

further promoted by the P-filling in the vacancies. The P-Co_3O_4 catalyst exhibited outstanding OER performance, with a η_{10} of 280 mV and a Tafel slope of 51.6 mV dec^{-1}.

3.1.4 The regulation of intercalated anions in layered double hydroxides (LDHs). In the cases discussed above, the anion regulations were performed inside the crystal structures. In other words, the regulated anions were connected with the metal ions by ionic bonds. Herein, a special form of anion regulation is introduced. Intercalated compounds are layered materials in which molecules or ions are inserted into the interlayer spaces. Layered double hydroxides (LDHs) are multi-metal hydroxides with anions intercalated between the hydroxide layers. LDH materials containing transition metal ions such as Fe, Co, Ni, and Mn have been identified as efficient OER catalysts.[38,47,48,136–148] In addition to the morphological control and cation regulation of the LDHs, the intercalated anions are also an important part of LDHs, and their OER activity can be improved by regulating the intercalated anions.

Müller et al. explored the role of intercalated anions in the OER activity of NiFe LDHs.[149] Through pulsed-laser ablation in liquids (PLAL) or by anion exchange, a series of anions were inserted between the layers of NiFe LDHs, including NO_3^-, BF_4^-, Cl^-, ClO_4^-, PO_4^{3-}, and CO_3^{2-}. The OER activities of the LDHs with different intercalated anions were measured, and several features were investigated to determine the factors that were critical to the OER performance. The basal spacings of LDH nanosheets varied with different interlayer anions. However, there was no significant correlation between the basal spacing and the OER overpotential. The OER activity was correlated with the basicity of the interlayer anions. Anions with higher pK_a values of their conjugate acids induced higher OER activity, which is attributed to the strong electron donating feature of the Lewis basic anions. Consequently, electrons can fill the empty orbits of the metal ions, facilitating the desorption of O_2. Moreover, as the intercalated ions are not as close to the metal ions, the interaction is relatively weak, and the adsorption of hydroxyl is not greatly weakened. Therefore, the OER activity did not decrease with high basicity of the interlayer anions.

The OER performance of phosphorus oxoanion-intercalated NiFe LDHs was reported by Sun et al.[150] Common LDH materials synthesized with urea as the alkaline source were intercalated with CO_3^{2-}, denoted as CO_3^{2-}/NiFe-LDH. Phosphorus oxoanion-intercalated NiFe LDHs were obtained in the presence of phosphate, phosphite, or hypophosphite, and the products were named PO_4^{3-}/NiFe-LDH, HPO_3^{2-}/NiFe-LDH, and $H_2PO_2^-$/NiFe-LDH, respectively. TEM images of the NiFe LDHs with different intercalated anions are shown in Fig. 7a–d. The major factor that affected the OER activity is the electronic structure of the Ni ions. As shown by the XPS results (Fig. 7e and f), when different anions were intercalated, the positions of the Ni $2p_{3/2}$ peaks were different. Hypophosphite, with the lowest P 2p binding energy, is a stronger electron donor than phosphate and phosphite. Thus, $H_2PO_2^-$/NiFe-LDH showed the lowest Ni oxidation state. From the above work reported by Müller et al.,[149] $H_2PO_2^-$/NiFe-LDH was

This journal is © the Partner Organisations 2018
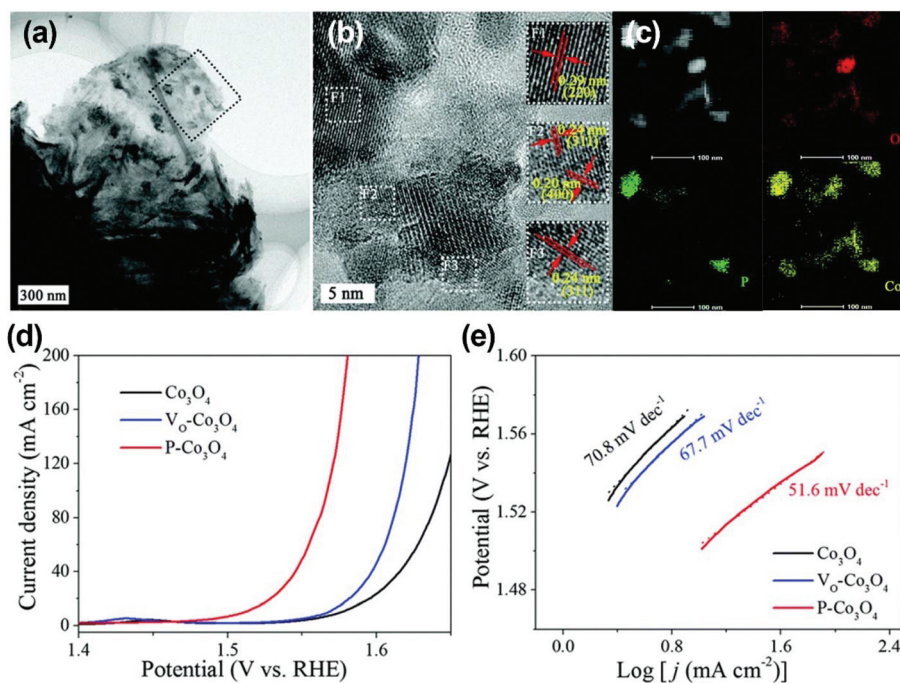
Inorg. Chem. Front., 2018, **5**, 521–534 | **527**

Fig. 6 Anion regulation of oxygen and phosphors in phosphors-filled vacancy-rich Co_3O_4. (a) TEM image of P-Co_3O_4. (b) HRTEM image of P-Co_3O_4. (c) EDS elemental mapping of the framed area in (a). (d) OER LSV plots and (e) OER Tafel plots of pristine Co_3O_4, vacancy-rich Co_3O_4, and P-filled Co_3O_4 in 1.0 M KOH.[135] Copyright 2017 Royal Society of Chemistry.
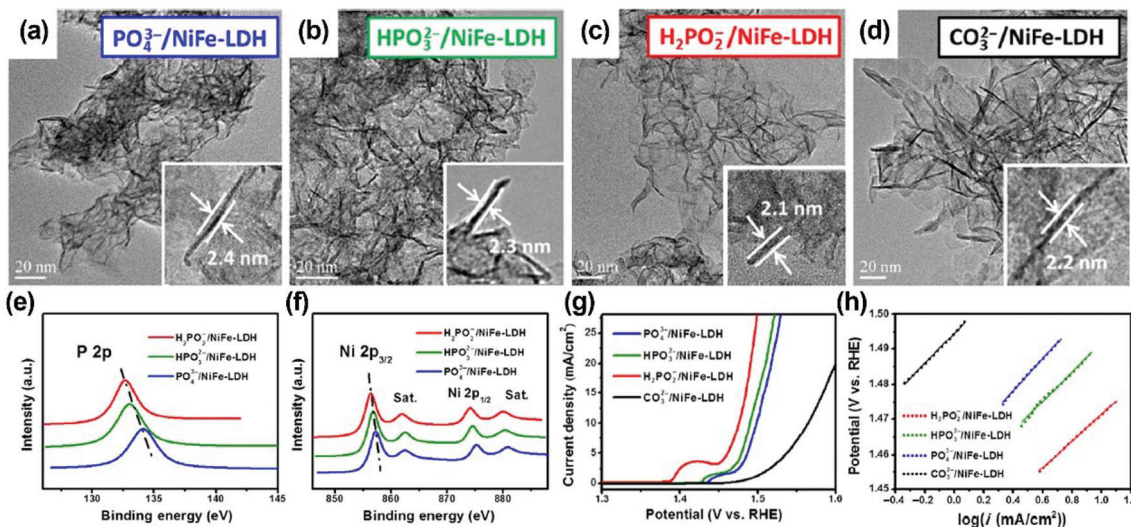

Fig. 7 Anion regulation of the intercalated anions in layered double hydroxides. (a)–(d) TEM images of NiFe LDHs with different intercalated anions. (e) P 2p and (f) Ni 2p high resolution XPS spectra of phosphorus oxoanion-intercalated NiFe LDHs. (g) OER LSV plots and (h) OER Tafel plots of phosphorus oxoanion and carbonate ion-intercalated NiFe LDHs in 1.0 M KOH with a scan rate of 1.0 mV s^{-1}.[150] Copyright 2017 Springer.

expected to possess the best OER activity. The OER LSV plots and Tafel plots are shown in Fig. 7g and 7h, respectively. The OER activity was arranged in the following order: $H_2PO_2^-$/NiFe-LDH > HPO_3^{2-}/NiFe-LDH > PO_4^{3-}/NiFe-LDH. This is in good agreement with the conclusions in Müller's work.[149]

The regulation of the intercalated ions of LDHs can be classified as a special type of anion regulation; it has also been performed using molybdate ions, alkoxide ions, etc.[151–155] Compared with anion regulation inside the crystal structure, intercalated anion regulation exhibits similar effects on OER activity; however, is more moderate and has less influence on the crystal structure. Studies on regulating the intercalated ions will aid the development of LDH materials for energy storage applications.

528 | *Inorg. Chem. Front.*, 2018, **5**, 521–534

This journal is © the Partner Organisations 2018

3.2 Oxygen-free transition metal compounds

Oxygen-free multi-anion transition metal compounds, usually containing chalcogens, nitrogen or phosphorus, have been mainly investigated as HER electrocatalysts or photocatalysts.[156–164] Since 2013, starting with sulfides,[165,166] emerging research on transition metal chalcogenides, nitrides, and phosphides for OER electrocatalysis has been reported. Anion regulation was also demonstrated as an efficient strategy to improve the activity in several studies.

In 2016, Wang *et al.* proposed an etched and N-doped Co_9S_8/graphene (N-Co_9S_8/G) hybrid for oxygen electrocatlaysis.[167] As with the synthesis of P-doped Co_3O_4,[135] the N-doped sulfide was obtained under plasma treatment. The as-prepared Co_9S_8/G was treated in NH_3-plasma at 700 °C for 1.0 h; then, defects and N dopants were generated in both the sulfide and graphene. This is the first report of N-doped sulfides for oxygen electrocatalysis. In the TEM image of N-Co_9S_8/G, shown in Fig. 8a, the partially etched Co_9S_8 and graphene can be observed. The lattice fringes with a *d*-spacing of 0.29 nm in the

HRTEM image (Fig. 8b) were attributed to the (311) plane of Co_9S_8, indicating that the crystal structure was maintained. The XPS survey and high-resolution Co 2p spectrum are shown in Fig. 8c and d, respectively. The signal at 398.33 eV corresponds to N element, and the peak at 780.3 eV in the Co 2p spectrum can be identified as the Co–N_x structure. The XPS results confirmed that N atoms were doped in the Co_9S_8 lattice. Due to the defects and N-doping in Co_9S_8, the OER activity of N-Co_9S_8/G surpassed that of Co_9S_8/G (Fig. 8e). The η_{10} of N-Co_9S_8/G (0.409 V) was the lowest among the sulfide samples and was close to that of RuO_2 (0.380 V, Fig. 8f). The OER activity of N-Co_9S_8/G was attributed to both the anion regulation of N/S and the defects generated by plasma etching. A Co_9S_8/G material treated under NH_3 flow at high temperature without plasma assistance was also synthesized and was denoted as NA-Co_9S_8/G. From the OER test results in Fig. 8e and f, the performance of NA-Co_9S_8/G was enhanced after N-doping, verifying the role of anion regulation.

The anion regulation of P and S in a nickel phosphosulphide water splitting electrocatalyst was recently reported by
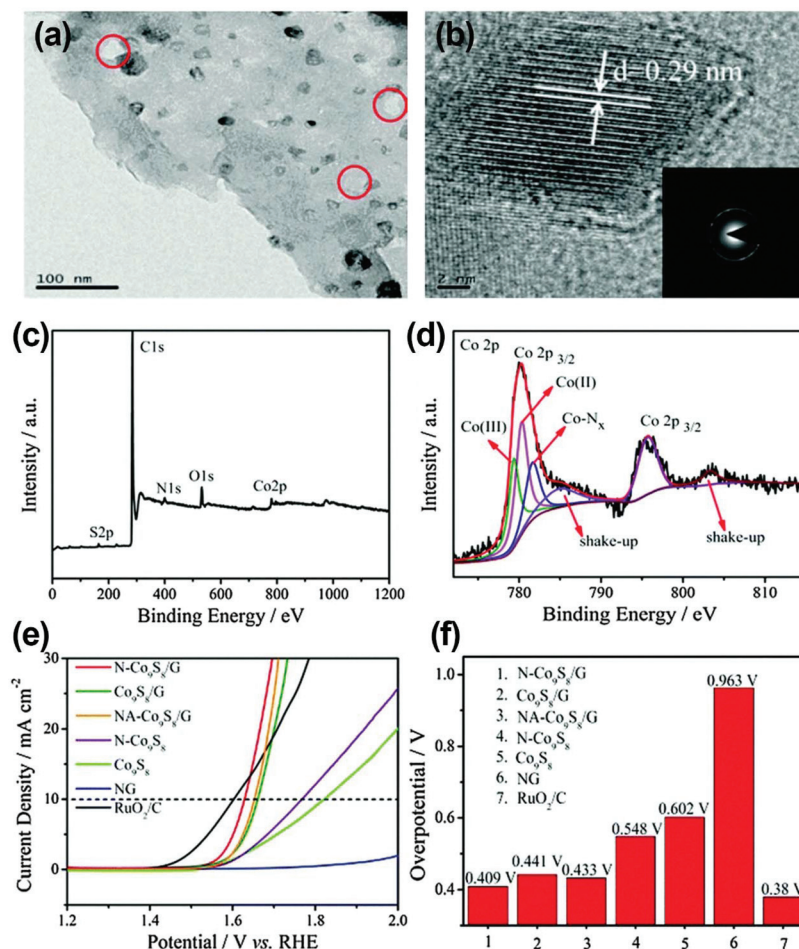

Fig. 8 Anion regulation of sulfur and nitrogen in nitrogen-doped Co_9S_8. (a) TEM image of N-Co_9S_8 supported on graphene material. (b) HRTEM image and selected area electron diffraction (SAED) pattern (inset) of N-Co_9S_8/G. (c) XPS survey of N-Co_9S_8/G. (d) High-resolution Co 2p XPS spectrum of N-Co_9S_8/G. (e) OER LSV plots tested at a scan rate of 10 mV s^{-1} in O_2-saturated 0.1 M KOH. (f) Overpotentials of the tested catalysts at 10 mA cm^{-2} OER current dronsity.[167] Copyright 2016 Royal Society of Chemistry.

This journal is © the Partner Organisations 2018

Inorg. Chem. Front., 2018, **5**, 521–534 | 529

Luo and Su *et al.*[168] A series of nickel phosphosulphides with different P/S ratios was synthesized, denoted as $NiP_{0.62}S_{0.38}$, $NiP_{0.45}S_{0.55}$, NiP, and NiS. Among these catalysts, $NiP_{0.62}S_{0.38}$ showed the highest activity, with an OER η_{10} of 240 mV (on Ni foam substrate). This anion-regulated phosphosulphide also exhibited excellent performance in overall water splitting. It is expected that as increasing studies are performed on transition metal chalcogenides, nitrides, and phosphides as OER electrocatalysts, the anion regulation of these materials will attract increasing attention.

4. Summary and outlook

Anion regulation on multi-anion transition metal compounds is an emerging strategy to design efficient OER electrocatalysts. The intrinsic activity of the metal cation active sites can be improved by regulating the adjacent anions. In addition to the anions introduced in this review, other anions, such as halide ions, oxyanions, and boron ions, can also be applied in anion regulation to enhance electrocatalytic activity.[169–171] With different adjacent anions, the electronic structures of the metal ions are modulated; then, the interactions between the active sites and the reactants, intermediates, and products are strengthened or weakened, resulting in changes in the OER activity. By anion regulation, including regulation of the types and ratio of the anions, the OER activity of transition metal compounds can be optimized.

Anion regulation usually refers to modifications inside the crystal lattice, and different anions are mixed at an atomic level. Meanwhile, there are some reports of OER catalysts fabricated by combining metal compound nanoparticles containing different anions or by forming core–shell structures.[122,123,172–177] At the interface of the two materials, the electronic structures of the metal ions are influenced by two different anions. The mechanism for enhancing the OER activity is similar to that of anion regulation. Design strategies of transition metal compound OER catalysts focusing on anions also include the total substitution of one type of anion with another,[84,87,178,179] the etching of anions to form vacancies,[180–185] *etc.* The interactions between the metal ions and adjacent anions can also be altered by these methods. These studies indicate that anions play important roles in the activity of transition metal compound OER catalysts, and new catalyst design strategies can be derived from the anion regulation method.

Although anion regulation has been successfully applied in many systems, the theoretical studies are not adequate to clearly and quantificationally describe the regulation process. Currently, possible mechanisms are simply being proposed and then confirmed by experimental results. For further investigations on anion regulation, advanced *in situ* or *in operando* techniques and theoretical analyses are both required to obtain deeper insights and better instructions for future developments. For example, intensive studies on oxygen incorporation in OER catalysts during electrochemical tests and the activity changes during the anion regulation process are strongly anticipated.

Anion regulation is an efficient method to improve the intrinsic activity of an electrocatalyst. Other methods can be applied to regulate the intrinsic activity, including cation regulation, combining two kinds of active sites (synergistic effects), and strain engineering.[186,187] The apparent activity of a catalyst depends not only on the intrinsic activity of the active sites, but also on the accessibility of the active sites – in other words, the number of effective active sites. The accessibility of the active sites is influenced by the pore structure, surface area, hydrophilicity, electrical conductivity of the catalyst, *etc*. With a well-designed structure, the mass transfer resistance can be decreased. The electrons in the electrode can easily reach the active sites when the electrocatalyst possesses good electrical conductivity. Consequently, more active sites are accessible and are involved in the reaction, leading to higher electrocatalytic activity. The implementation of anion regulation should be combined with other design strategies to obtain the best catalyst activity.

The need for advanced energy storage and conversion materials continues to increase. With comprehensive and in-depth understanding of anion regulation, together with other material design strategies, the development of new energy materials can reach a higher level. It is expected that with continuous research on anion regulation, highly active energy electrocatalysts can be realized and will play an important role in the energy field in the future.

Conflicts of interest

There are no conflicts to declare.

Acknowledgements

References

1 S. Chu and A. Majumdar, *Nature*, 2012, **488**, 294–303.

2 X. M. Li, X. G. Hao, A. Abudula and G. Q. Guan, *J. Mater. Chem. A*, 2016, **4**, 11973–12000.

3 D. J. Yang, L. J. Zhang, X. C. Yan and X. D. Yao, *Small Methods*, 2017, **1**, 1700209.

4 Y. Jiao, Y. Zheng, M. T. Jaroniec and S. Z. Qiao, *Chem. Soc. Rev.*, 2015, **44**, 2060–2086.

5 J. S. Lee, S. T. Kim, R. Cao, N. S. Choi, M. Liu, K. T. Lee and J. Cho, *Adv. Energy Mater.*, 2011, **1**, 34–50.

6 Y. G. Li and H. J. Dai, *Chem. Soc. Rev.*, 2014, **43**, 5257–5275.

7 W. Chen, Y. F. Gong and J. H. Liu, *Chin. Chem. Lett.*, 2017, **28**, 709–718.

8 N. T. Suen, S. F. Hung, Q. Quan, N. Zhang, Y. J. Xu and H. M. Chen, *Chem. Soc. Rev.*, 2017, **46**, 337–365.

9 M. Gong and H. J. Dai, *Nano Res.*, 2015, **8**, 23–39.

10 H. Over, *Chem. Rev.*, 2012, **112**, 3356–3426.

11 Y. Lee, J. Suntivich, K. J. May, E. E. Perry and Y. Shao-Horn, *J. Phys. Chem. Lett.*, 2012, **3**, 399–404.

12 L. Han, S. J. Dong and E. K. Wang, *Adv. Mater.*, 2016, **28**, 9266–9291.

13 J. H. Wang, W. Cui, Q. Liu, Z. C. Xing, A. M. Asiri and X. P. Sun, *Adv. Mater.*, 2016, **28**, 215–230.

14 H. Osgood, S. V. Devaguptapu, H. Xu, J. Cho and G. Wu, *Nano Today*, 2016, **11**, 601–625.

15 F. M. Wang, T. A. Shifa, X. Y. Zhan, Y. Huang, K. L. Liu, Z. Z. Cheng, C. Jiang and J. He, *Nanoscale*, 2015, **7**, 19764–19788.

16 X. Q. Zhang, X. B. Cheng and Q. Zhang, *J. Energy Chem.*, 2016, **25**, 967–984.

17 G. L. Tian, Q. Zhang, B. S. Zhang, Y. G. Jin, J. Q. Huang, D. S. Su and F. Wei, *Adv. Funct. Mater.*, 2014, **24**, 5956–5961.

18 C. Tang, H. F. Wang, X. Chen, B. Q. Li, T. Z. Hou, B. S. Zhang, Q. Zhang, M. M. Titirici and F. Wei, *Adv. Mater.*, 2016, **28**, 6845–6851.

19 W. Zhang, W. Z. Lai and R. Cao, *Chem. Rev.*, 2017, **117**, 3717–3797.

20 C. Tang, M. M. Titirici and Q. Zhang, *J. Energy Chem.*, 2017, **26**, 1077–1093.

21 G. L. Tian, M. Q. Zhao, D. S. Yu, X. Y. Kong, J. Q. Huang, Q. Zhang and F. Wei, *Small*, 2014, **10**, 2251–2259.

22 M. Li, Z. W. Liu, F. Wang and J. J. Xuan, *J. Energy Chem.*, 2017, **26**, 422–427.

23 Y. C. Tu, D. H. Deng and X. H. Bao, *J. Energy Chem.*, 2016, **25**, 957–966.

24 H. H. Wu, X. L. Jiang, Y. F. Ye, C. C. Yan, S. H. Xie, S. Miao, G. X. Wang and X. H. Bao, *J. Energy Chem.*, 2017, **26**, 1181–1186.

25 M. Z. Yu, S. Zhou, Y. Liu, Z. Y. Wang, T. Zhou, J. J. Zhao, Z. B. Zhao and J. S. Qiu, *Sci. China Mater.*, 2017, **60**, 415–426.

26 S. Cobo, J. Heidkamp, P. A. Jacques, J. Fize, V. Fourmond, L. Guetaz, B. Jousselme, V. Ivanova, H. Dau, S. Palacin, M. Fontecave and V. Artero, *Nat. Mater.*, 2012, **11**, 802–807.

27 A. Singh and L. Spiccia, *Coord. Chem. Rev.*, 2013, **257**, 2607–2622.

28 H. Ooka, T. Takashima, A. Yamaguchi, T. Hayashi and R. Nakamura, *Chem. Commun.*, 2017, **53**, 7149–7161.

29 Z. W. Seh, J. Kibsgaard, C. F. Dickens, I. B. Chorkendorff, J. K. Norskov and T. F. Jaramillo, *Science*, 2017, **355**, eaad4998.

30 C. Tang, H. F. Wang and Q. Zhang, *Acc. Chem. Res.*, 2018, DOI: 10.1021/acs.accounts.1027b00616.

31 J. H. Montoya, L. C. Seitz, P. Chakthranont, A. Vojvodic, T. F. Jaramillo and J. K. Norskov, *Nat. Mater.*, 2017, **16**, 70–81.

32 B. Q. Li, S. Y. Zhang, C. Tang, X. Y. Cui and Q. Zhang, *Small*, 2017, **13**, 1700610.

33 M. S. Burke, M. G. Kast, L. Trotochaud, A. M. Smith and S. W. Boettcher, *J. Am. Chem. Soc.*, 2015, **137**, 3638–3648.

34 D. Friebel, M. W. Louie, M. Bajdich, K. E. Sanwald, Y. Cai, A. M. Wise, M. J. Cheng, D. Sokaras, T. C. Weng, R. Alonso-Mori, R. C. Davis, J. R. Bargar, J. K. Norskov, A. Nilsson and A. T. Bell, *J. Am. Chem. Soc.*, 2015, **137**, 1305–1313.

35 L. Trotochaud, S. L. Young, J. K. Ranney and S. W. Boettcher, *J. Am. Chem. Soc.*, 2014, **136**, 6744–6753.

36 C. Tang, H. F. Wang, H. S. Wang, F. Wei and Q. Zhang, *J. Mater. Chem. A*, 2016, **4**, 3210–3216.

37 S. Anantharaj, S. R. Ede, K. Sakthikumar, K. Karthick, S. Mishra and S. Kundu, *ACS Catal.*, 2016, **6**, 8069–8097.

38 M. Gong, Y. G. Li, H. L. Wang, Y. Y. Liang, J. Z. Wu, J. G. Zhou, J. Wang, T. Regier, F. Wei and H. J. Dai, *J. Am. Chem. Soc.*, 2013, **135**, 8452–8455.

39 M. W. Louie and A. T. Bell, *J. Am. Chem. Soc.*, 2013, **135**, 12329–12337.

40 M. Gong, D. Y. Wang, C. C. Chen, B. J. Hwang and H. J. Dai, *Nano Res.*, 2016, **9**, 28–46.

41 Y. Gao, F. X. Wu and H. Chen, *J. Energy Chem.*, 2017, **26**, 428–432.

42 A. R. Jadhav, H. A. Bandal, A. H. Tamboli and H. Kim, *J. Energy Chem.*, 2017, **26**, 695–702.

43 C. Tang, B. Wang, H. F. Wang and Q. Zhang, *Adv. Mater.*, 2017, **29**, 1703185.

44 L. Wei, H. E. Karahan, S. L. Zhai, H. W. Liu, X. C. Chen, Z. Zhou, Y. J. Lei, Z. W. Liu and Y. Chen, *Adv. Mater.*, 2017, **29**, 1701410.

45 S. L. Yang, T. R. Zhang, G. C. Li, L. Q. Yang and J. Y. Lee, *Energy Storage Mater.*, 2017, **6**, 140–148.

46 X. L. Zhao, W. Zhang and R. Cao, *J. Energy Chem.*, 2017, **26**, 1210–1216.

47 L. Zhou, M. F. Shao, M. Wei and X. Duan, *J. Energy Chem.*, 2017, **26**, 1094–1106.

48 X. L. Zhu, C. Tang, H. F. Wang, B. Q. Li, Q. Zhang, C. Y. Li, C. H. Yang and F. Wei, *J. Mater. Chem. A*, 2016, **4**, 7245–7250.

49 B. Q. Li, C. Tang, H. F. Wang, X. L. Zhu and Q. Zhang, *Sci. Adv.*, 2016, **2**, e1600495.

50 F. Zhang, Y. M. Shi, T. Xue, J. F. Zhang, Y. Liang and B. Zhang, *Sci. China Mater.*, 2017, **60**, 324–334.

51 J. L. Meng, J. Q. Fu, X. X. Yang, M. J. Wei, S. Liang, H. Y. Zang, H. Q. Tan, Y. H. Wang and Y. G. Li, *Inorg. Chem. Front.*, 2017, **4**, 1791–1797.

52 G. Wan, C. Yang, W. P. Zhao, Q. R. Li, N. Wang, T. Li, H. Zhou, H. R. Chen and J. L. Shi, *Adv. Mater.*, 2017, **29**, 1703436.

53 B. Q. Li, Z. J. Xia, B. S. Zhang, C. Tang, H. F. Wang and Q. Zhang, *Nat. Commun.*, 2017, **8**, 934.

54 J. Y. C. Chen, J. T. Miller, J. B. Gerken and S. S. Stahl, *Energy Environ. Sci.*, 2014, **7**, 1382–1386.

55 Y. C. Pi, Q. Shao, P. T. Wang, F. Lv, S. J. Guo, J. Guo and X. Q. Huang, *Angew. Chem., Int. Ed.*, 2017, **56**, 4502–4506.

This journal is © the Partner Organisations 2018

Inorg. Chem. Front., 2018, **5**, 521–534 | 531

56 B. Zhang, X. L. Zheng, O. Voznyy, R. Comin, M. Bajdich, M. Garcia-Melchor, L. L. Han, J. X. Xu, M. Liu, L. R. Zheng, F. P. G. de Arquer, C. T. Dinh, F. J. Fan, M. J. Yuan, E. Yassitepe, N. Chen, T. Regier, P. F. Liu, Y. H. Li, P. De Luna, A. Janmohamed, H. L. L. Xin, H. G. Yang, A. Vojvodic and E. H. Sargent, *Science*, 2016, **352**, 333–337.

57 T. N. Huan, G. Rousse, S. Zanna, I. T. Lucas, X. Z. Xu, N. Menguy, V. Mougel and M. Fontecave, *Angew. Chem., Int. Ed.*, 2017, **56**, 4792–4796.

58 M. Risch, K. Klingan, F. Ringleb, P. Chernev, I. Zaharieva, A. Fischer and H. Dau, *ChemSusChem*, 2012, **5**, 542–549.

59 S. Dey, B. Mondal and A. Dey, *Phys. Chem. Chem. Phys.*, 2014, **16**, 12221–12227.

60 B. Ananthoju, J. Mohapatra, M. K. Jangid, D. Bahadur, N. V. Medhekar and M. Aslam, *Sci. Rep.*, 2016, **6**, 35369.

61 H. J. Yin and Z. Y. Tang, *Chem. Soc. Rev.*, 2016, **45**, 4873–4891.

62 Y. Zhang, Q. Zhou, J. X. Zhu, Q. Y. Yan, S. X. Dou and W. P. Sun, *Adv. Funct. Mater.*, 2017, **27**, 1702317.

63 H. Yuan, L. Kong, T. Li and Q. Zhang, *Chin. Chem. Lett.*, 2017, **28**, 2180–2194.

64 J. F. Xie and Y. Xie, *Chem. – Eur. J.*, 2016, **22**, 3588–3598.

65 Y. Lv and X. B. Wang, *Catal. Sci. Technol.*, 2017, **7**, 3676–3691.

66 Y. Wang, B. Kong, D. Y. Zhao, H. T. Wang and C. Selomulya, *Nano Today*, 2017, **15**, 26–55.

67 S. Jin, *ACS Energy Lett.*, 2017, **2**, 1937–1938.

68 T. Y. Ma, S. Dai, M. Jaroniec and S. Z. Qiao, *J. Am. Chem. Soc.*, 2014, **136**, 13925–13931.

69 J. A. Koza, Z. He, A. S. Miller and J. A. Switzer, *Chem. Mater.*, 2012, **24**, 3567–3573.

70 J. Rosen, G. S. Hutchings and F. Jiao, *J. Am. Chem. Soc.*, 2013, **135**, 4516–4521.

71 Y. J. Sa, K. Kwon, J. Y. Cheon, F. Kleitz and S. H. Joo, *J. Mater. Chem. A*, 2013, **1**, 9992–10001.

72 H. Tuysuz, Y. J. Hwang, S. B. Khan, A. M. Asiri and P. D. Yang, *Nano Res.*, 2013, **6**, 47–54.

73 J. Wu, Y. Xue, X. Yan, W. S. Yan, Q. M. Cheng and Y. Xie, *Nano Res.*, 2012, **5**, 521–530.

74 A. Bergmann, E. Martinez-Moreno, D. Teschner, P. Chernev, M. Gliech, J. F. de Araujo, T. Reier, H. Dau and P. Strasser, *Nat. Commun.*, 2015, **6**, 8625.

75 M. Bajdich, M. Garcia-Mota, A. Vojvodic, J. K. Norskov and A. T. Bell, *J. Am. Chem. Soc.*, 2013, **135**, 13521–13530.

76 H. Y. Wang, S. F. Hung, H. Y. Chen, T. S. Chan, H. M. Chen and B. Liu, *J. Am. Chem. Soc.*, 2016, **138**, 36–39.

77 D. Friebel, M. Bajdich, B. S. Yeo, M. W. Louie, D. J. Miller, H. S. Casalongue, F. Mbuga, T. C. Weng, D. Nordlund, D. Sokaras, R. Alonso-Mori, A. T. Bell and A. Nilsson, *Phys. Chem. Chem. Phys.*, 2013, **15**, 17460–17467.

78 L. J. Enman, M. S. Burke, A. S. Batchellor and S. W. Boettcher, *ACS Catal.*, 2016, **6**, 2416–2423.

79 F. Dionigi and P. Strasser, *Adv. Energy Mater.*, 2016, **6**, 1600621.

80 J. H. Huang, J. T. Chen, T. Yao, J. F. He, S. Jiang, Z. H. Sun, Q. H. Liu, W. R. Cheng, F. C. Hu, Y. Jiang, Z. Y. Pan and S. Q. Wei, *Angew. Chem., Int. Ed.*, 2015, **54**, 8722–8727.

81 M. S. Burke, S. H. Zou, L. J. Enman, J. E. Kellon, C. A. Gabor, E. Pledger and S. W. Boettcher, *J. Phys. Chem. Lett.*, 2015, **6**, 3737–3742.

82 L. D. Wang, D. Mitoraj, S. Turner, O. V. Khavryuchenko, T. Jacob, R. K. Hocking and R. Beranek, *ACS Catal.*, 2017, **7**, 4759–4767.

83 P. T. Babar, B. S. Pawar, A. C. Lokhande, M. G. Gang, J. S. Jang, M. P. Suryawanshi, S. M. Pawar and J. H. Kim, *J. Energy Chem.*, 2017, **26**, 757–761.

84 W. Chen, H. T. Wang, Y. Z. Li, Y. Y. Liu, J. Sun, S. H. Lee, J. S. Lee and Y. Cui, *ACS Cent. Sci.*, 2015, **1**, 244–251.

85 A. Dutta, A. K. Samantara, S. K. Dutta, B. K. Jena and N. Pradhan, *ACS Energy Lett.*, 2016, **1**, 169–174.

86 H. Liang, A. N. Gandi, C. Xia, M. N. Hedhili, D. H. Anjum, U. Schwingenschlogl and H. N. Alshareef, *ACS Energy Lett.*, 2017, **2**, 1035–1042.

87 O. Mabayoje, A. Shoola, B. R. Wygant and C. B. Mullins, *ACS Energy Lett.*, 2016, **1**, 195–201.

88 L. A. Stern, L. G. Feng, F. Song and X. L. Hu, *Energy Environ. Sci.*, 2015, **8**, 2347–2351.

89 X. Xu, F. Song and X. L. Hu, *Nat. Commun.*, 2016, **7**, 12324.

90 E. Y. Zhao, X. Q. Yu, F. W. Wang and H. Li, *Sci. China: Chem.*, 2017, **60**, 1483–1493.

91 J. S. Chen, J. W. Ren, M. Shalom, T. Fellinger and M. Antoniettit, *ACS Appl. Mater. Interfaces*, 2016, **8**, 5509–5516.

92 J. Zhang, T. Wang, D. Pohl, B. Rellinghaus, R. H. Dong, S. H. Liu, X. D. Zhuang and X. L. Feng, *Angew. Chem., Int. Ed.*, 2016, **55**, 6702–6707.

93 J. Wang, H. X. Zhong, Z. L. Wang, F. L. Meng and X. B. Zhang, *ACS Nano*, 2016, **10**, 2342–2348.

94 C. Xia, Q. Jiang, C. Zhao, M. N. Hedhili and H. N. Alshareef, *Adv. Mater.*, 2016, **28**, 77–85.

95 W. X. Zhu, X. Y. Yue, W. T. Zhang, S. X. Yu, Y. H. Zhang, J. Wang and J. L. Wang, *Chem. Commun.*, 2016, **52**, 1486–1489.

96 A. T. Swesi, J. Masud and M. Nath, *Energy Environ. Sci.*, 2016, **9**, 1771–1782.

97 J. W. Nai, Y. Lu, L. Yu, X. Wang and X. W. Lou, *Adv. Mater.*, 2017, **29**, 1703870.

98 S. L. Zhao, Y. Wang, Q. H. Zhang, Y. F. Li, L. Gu, Z. H. Dai, S. L. Liu, Y. Q. Lan, M. Han and J. C. Bao, *Inorg. Chem. Front.*, 2016, **3**, 1501–1509.

99 H. L. Zhu, R. Jiang, X. Q. Chen, Y. G. Chen and L. Y. Wang, *Sci. Bull.*, 2017, **62**, 1373–1379.

100 P. Z. Chen, T. P. Zhou, M. X. Zhang, Y. Tong, C. G. Zhong, N. Zhang, L. D. Zhang, C. Z. Wu and Y. Xie, *Adv. Mater.*, 2017, **29**, 1701584.

101 X. C. Duan, J. T. Xu, Z. X. Wei, J. M. Ma, S. J. Guo, H. K. Liu and S. X. Dou, *Small Methods*, 2017, **1**, 1700156.

532 | *Inorg. Chem. Front.*, 2018, **5**, 521–534

This journal is © the Partner Organisations 2018

102 H. F. Wang, C. Tang, B. Wang, B. Q. Li and Q. Zhang, *Adv. Mater.*, 2017, **29**, 1702327.

103 P. W. Cai, J. H. Huang, J. X. Chen and Z. H. Wen, *Angew. Chem., Int. Ed.*, 2017, **56**, 4858–4861.

104 J. F. Zhang, Y. C. Hu, D. L. Liu, Y. Yu and B. Zhang, *Adv. Sci.*, 2017, **4**, 1600343.

105 J. Fu, F. M. Hassan, C. Zhong, J. Lu, H. Liu, A. P. Yu and Z. W. Chen, *Adv. Mater.*, 2017, **29**, 1702526.

106 K. Maeda and K. Domen, *Angew. Chem., Int. Ed.*, 2012, **51**, 9865–9869.

107 B. Siritanaratkul, K. Maeda, T. Hisatomi and K. Domen, *ChemSusChem*, 2011, **4**, 74–78.

108 M. Higashi, K. Domen and R. Abe, *J. Am. Chem. Soc.*, 2012, **134**, 6968–6971.

109 K. Ueda, T. Minegishi, J. Clune, M. Nakabayashi, T. Hisatomi, H. Nishiyama, M. Katayama, N. Shibata, J. Kubota, T. Yamada and K. Domen, *J. Am. Chem. Soc.*, 2015, **137**, 2227–2230.

110 X. B. Chen, Y. B. Lou, A. C. S. Samia, C. Burda and J. L. Gole, *Adv. Funct. Mater.*, 2005, **15**, 41–49.

111 G. Hitoki, T. Takata, J. N. Kondo, M. Hara, H. Kobayashi and K. Domen, *Chem. Commun.*, 2002, 1698–1699.

112 K. Maeda, M. Higashi, D. L. Lu, R. Abe and K. Domen, *J. Am. Chem. Soc.*, 2010, **132**, 5858–5868.

113 Y. Q. Li, A. C. A. Delsing, G. de With and H. T. Hintzen, *Chem. Mater.*, 2005, **17**, 3242–3248.

114 R. J. Xie, N. Hirosaki, M. Mitomo, K. Sakuma and N. Kimura, *Appl. Phys. Lett.*, 2006, **89**, 3.

115 Y. Li, K. A. Kuttiyiel, L. J. Wu, Y. M. Zhu, E. Fujita, R. R. Adzic and K. Sasaki, *ChemSusChem*, 2017, **10**, 68–73.

116 M. Shalom, D. Ressnig, X. F. Yang, G. Clavel, T. P. Fellinger and M. Antonietti, *J. Mater. Chem. A*, 2015, **3**, 8171–8177.

117 K. Xu, P. Z. Chen, X. L. Li, Y. Tong, H. Ding, X. J. Wu, W. S. Chu, Z. M. Peng, C. Z. Wu and Y. Xie, *J. Am. Chem. Soc.*, 2015, **137**, 4119–4125.

118 Y. Q. Zhang, B. Ouyang, J. Xu, G. C. Jia, S. Chen, R. S. Rawat and H. J. Fan, *Angew. Chem., Int. Ed.*, 2016, **55**, 8670–8674.

119 Y. Y. Wang, C. Xie, D. D. Liu, X. B. Huang, J. Huo and S. Y. Wang, *ACS Appl. Mater. Interfaces*, 2016, **8**, 18652–18657.

120 B. Zhang, C. H. Xiao, S. M. Xie, J. Liang, X. Chen and Y. H. Tang, *Chem. Mater.*, 2016, **28**, 6934–6941.

121 P. Z. Chen, K. Xu, Y. Tong, X. L. Li, S. Tao, Z. W. Fang, W. S. Chu, X. J. Wu and C. Z. Wu, *Inorg. Chem. Front.*, 2016, **3**, 236–242.

122 J. Yin, Y. X. Li, F. Lv, Q. H. Fan, Y. Q. Zhao, Q. L. Zhang, W. Wang, F. Y. Cheng, P. X. Xi and S. J. Guo, *ACS Nano*, 2017, **11**, 2275–2283.

123 P. Z. Chen, K. Xu, Z. W. Fang, Y. Tong, J. C. Wu, X. L. Lu, X. Peng, H. Ding, C. Z. Wu and Y. Xie, *Angew. Chem., Int. Ed.*, 2015, **54**, 14710–14714.

124 B. You, N. Jiang, M. L. Sheng, M. W. Bhushan and Y. J. Sun, *ACS Catal.*, 2016, **6**, 714–721.

125 Y. P. Zhu, Y. P. Liu, T. Z. Ren and Z. Y. Yuan, *Adv. Funct. Mater.*, 2015, **25**, 7337–7347.

126 M. Ledendecker, S. K. Calderon, C. Papp, H. P. Steinruck, M. Antonietti and M. Shalom, *Angew. Chem., Int. Ed.*, 2015, **54**, 12361–12365.

127 X. Y. Yu, Y. Feng, B. Y. Guan, X. W. Lou and U. Paik, *Energy Environ. Sci.*, 2016, **9**, 1246–1250.

128 A. Han, H. L. Chen, Z. J. Sun, J. Xu and P. W. Du, *Chem. Commun.*, 2015, **51**, 11626–11629.

129 F. Hu, S. L. Zhu, S. M. Chen, Y. Li, L. Ma, T. P. Wu, Y. Zhang, C. M. Wang, C. C. Liu, X. J. Yang, L. Song, X. W. Yang and Y. J. Xiong, *Adv. Mater.*, 2017, **29**, 1606570.

130 X. Bai, Z. Y. Ren, S. C. Du, H. Y. Meng, J. Wu, Y. Z. Xue, X. J. Zhao and H. G. Fu, *Sci. Bull.*, 2017, **62**, 1510–1518.

131 M. Ma, D. Liu, S. Hao, R. M. Kong, G. Du, A. M. Asiri, Y. D. Yao and X. P. Sun, *Inorg. Chem. Front.*, 2017, **4**, 840–844.

132 J. T. Ren, Z. P. Hu, C. Chen, Y. P. Liu and Z. Y. Yuan, *J. Energy Chem.*, 2017, **26**, 1196–1202.

133 J. J. Duan, S. Chen, A. Vasileff and S. Z. Qiao, *ACS Nano*, 2016, **10**, 8738–8745.

134 Z. J. Li, X. Y. Dou, Y. C. Zhao and C. Z. Wu, *Inorg. Chem. Front.*, 2016, **3**, 1021–1027.

135 Z. Xiao, Y. Wang, Y.-C. Huang, Z. Wei, C.-L. Dong, J. Ma, S. Shen, Y. Li and S. Wang, *Energy Environ. Sci.*, 2017, **10**, 2563–2569.

136 W. Ma, R. Z. Ma, C. X. Wang, J. B. Liang, X. H. Liu, K. C. Zhou and T. Sasaki, *ACS Nano*, 2015, **9**, 1977–1984.

137 Z. Lu, W. W. Xu, W. Zhu, Q. Yang, X. D. Lei, J. F. Liu, Y. P. Li, X. M. Sun and X. Duan, *Chem. Commun.*, 2014, **50**, 6479–6482.

138 F. Song and X. L. Hu, *J. Am. Chem. Soc.*, 2014, **136**, 16481–16484.

139 H. F. Liang, F. Meng, M. Caban-Acevedo, L. S. Li, A. Forticaux, L. C. Xiu, Z. C. Wang and S. Jin, *Nano Lett.*, 2015, **15**, 1421–1427.

140 Z. Y. Lu, L. Qian, Y. Tian, Y. P. Li, X. M. Sun and X. Duan, *Chem. Commun.*, 2016, **52**, 908–911.

141 X. Long, Z. L. Wang, S. Xiao, Y. M. An and S. H. Yang, *Mater. Today*, 2016, **19**, 213–226.

142 C. Tang, H. S. Wang, H. F. Wang, Q. Zhang, G. L. Tian, J. Q. Nie and F. Wei, *Adv. Mater.*, 2015, **27**, 4516–4522.

143 H. F. Wang, C. Tang and Q. Zhang, *J. Mater. Chem. A*, 2015, **3**, 16183–16189.

144 X. L. Zhu, C. Tang, H. F. Wang, Q. Zhang, C. H. Yang and F. Wei, *J. Mater. Chem. A*, 2015, **3**, 24540–24546.

145 C. Tang, H. F. Wang, X. L. Zhu, B. Q. Li and Q. Zhang, *Part. Part. Syst. Charact.*, 2016, **33**, 473–486.

146 H. D. Yang, S. Luo, Y. Bao, Y. T. Luo, J. Jin and J. T. Ma, *Inorg. Chem. Front.*, 2017, **4**, 1173–1181.

147 C. Andronescu, S. Barwe, E. Ventosa, J. Masa, E. Vasile, B. Konkena, S. Moller and W. Schuhmann, *Angew. Chem., Int. Ed.*, 2017, **56**, 11258–11262.

148 Y. F. Zhao, B. Li, Q. Wang, W. Gao, C. L. J. Wang, M. Wei, D. G. Evans, X. Duan and D. O'Hare, *Chem. Sci.*, 2014, **5**, 951–958.

149 B. M. Hunter, W. Hieringer, J. R. Winkler, H. B. Gray and A. M. Müller, *Energy Environ. Sci.*, 2016, **9**, 1734–1743.

150 M. Luo, Z. Cai, C. Wang, Y. M. Bi, L. Qian, Y. C. Hao, L. Li, Y. Kuang, Y. P. Li, X. D. Lei, Z. Y. Huo, W. Liu, H. L. Wang, X. M. Sun and X. Duan, *Nano Res.*, 2017, **10**, 1732–1739.

151 J. A. Carrasco, J. Romero, M. Varela, F. Hauke, G. Abellan, A. Hirsch and E. Coronado, *Inorg. Chem. Front.*, 2016, **3**, 478–487.

152 N. Han, F. P. Zhao and Y. G. Li, *J. Mater. Chem. A*, 2015, **3**, 16348–16353.

153 C. Xie, Y. Y. Wang, K. Hu, L. Tao, X. B. Huang, J. Huo and S. Y. Wang, *J. Mater. Chem. A*, 2017, **5**, 87–91.

154 X. M. Li, X. G. Hao, Z. D. Wang, A. Abudula and G. Q. Guan, *J. Power Sources*, 2017, **347**, 193–200.

155 H. H. Zhong, R. Tian, X. M. Gong, D. Q. Li, P. G. Tang, N. Alonso-Vante and Y. J. Feng, *J. Power Sources*, 2017, **361**, 21–30.

156 D. Mukherjee, P. M. Austeria and S. Sampath, *ACS Energy Lett.*, 2016, **1**, 367–372.

157 W. Xiao, P. T. Liu, J. Y. Zhang, W. D. Song, Y. P. Feng, D. Q. Gao and J. Ding, *Adv. Energy Mater.*, 2017, **7**, 1602086.

158 J. Kibsgaard and T. F. Jaramillo, *Angew. Chem., Int. Ed.*, 2014, **53**, 14433–14437.

159 B. Konkena, J. Masa, W. Xia, M. Muhler and W. Schuhmann, *Nano Energy*, 2016, **29**, 46–53.

160 K. Wang, C. J. Zhou, D. Xi, Z. Q. Shi, C. He, H. Y. Xia, G. W. Liu and G. J. Qiao, *Nano Energy*, 2015, **18**, 1–11.

161 M. A. R. Anjum and J. S. Lee, *ACS Catal.*, 2017, **7**, 3030–3038.

162 Y. M. Xin, X. Kan, L. Y. Gan and Z. H. Zhang, *ACS Nano*, 2017, **11**, 10303–10312.

163 Y. Hou, M. Qiu, T. Zhang, X. D. Zhuang, C. S. Kim, C. Yuan and X. L. Feng, *Adv. Mater.*, 2017, **29**, 1701589.

164 K. C. Kwon, S. Choi, J. Lee, K. Hong, W. Sohn, D. M. Andoshe, K. S. Choi, Y. Kim, S. Han, S. Y. Kim and H. W. Jang, *J. Mater. Chem. A*, 2017, **5**, 15534–15542.

165 Q. Liu, J. T. Jin and J. Y. Zhang, *ACS Appl. Mater. Interfaces*, 2013, **5**, 5002–5008.

166 W. J. Zhou, X. J. Wu, X. H. Cao, X. Huang, C. L. Tan, J. Tian, H. Liu, J. Y. Wang and H. Zhang, *Energy Environ. Sci.*, 2013, **6**, 2921–2924.

167 S. Dou, L. Tao, J. Huo, S. Y. Wang and L. M. Dai, *Energy Environ. Sci.*, 2016, **9**, 1320–1326.

168 J. Luo, H. Y. Wang, G. Su, Y. L. Tang, H. Q. Liu, F. Y. Tian and D. L. Li, *J. Mater. Chem. A*, 2017, **5**, 14865–14872.

169 S. Wan, J. Qi, W. Zhang, W. Wang, S. Zhang, K. Liu, H. Zheng, J. Sun, S. Wang and R. Cao, *Adv. Mater.*, 2017, **29**, 1700286.

170 Y. Wang, W. Ding, S. G. Chen, Y. Nie, K. Xiong and Z. D. Wei, *Chem. Commun.*, 2014, **50**, 15529–15532.

171 J. Masa, P. Weide, D. Peeters, I. Sinev, W. Xia, Z. Y. Sun, C. Somsen, M. Muhler and W. Schuhmann, *Adv. Energy Mater.*, 2016, **6**, 10.

172 X. Zhong, Y. Jiang, X. L. Chen, L. Wang, G. L. Zhuang, X. N. Li and J. G. Wang, *J. Mater. Chem. A*, 2016, **4**, 10575–10584.

173 J. F. Chang, Y. Xiao, M. L. Xiao, J. J. Ge, C. P. Liu and W. Xing, *ACS Catal.*, 2015, **5**, 6874–6878.

174 J. Yang, G. X. Zhu, Y. J. Liu, J. X. Xia, Z. Y. Ji, X. P. Shen and S. K. Wu, *Adv. Funct. Mater.*, 2016, **26**, 4712–4721.

175 X. Q. Ji, X. Ren, S. Hao, F. Y. Xie, F. L. Qu, G. Du, A. M. Asiri and X. P. Sun, *Inorg. Chem. Front.*, 2017, **4**, 1546–1550.

176 S. J. Deng, S. H. Shen, Y. Zhong, K. L. Zhang, J. B. Wu, X. L. Wang, X. H. Xia and J. P. Tu, *J. Energy Chem.*, 2017, **26**, 1203–1209.

177 K. D. Li, J. F. Zhang, R. Wu, Y. F. Yu and B. Zhang, *Adv. Sci.*, 2016, **3**, 1500426.

178 X. D. Jia, Y. F. Zhao, G. B. Chen, L. Shang, R. Shi, X. F. Kang, G. I. N. Waterhouse, L. Z. Wu, C. H. Tung and T. R. Zhang, *Adv. Energy Mater.*, 2016, **6**, 1502585.

179 W. Chen, Y. Y. Liu, Y. Z. Li, J. Sun, Y. C. Qiu, C. Liu, G. M. Zhou and Y. Cui, *Nano Lett.*, 2016, **16**, 7588–7596.

180 R. Gao, Z. Y. Li, X. L. Zhang, J. C. Zhang, Z. B. Hu and X. F. Liu, *ACS Catal.*, 2016, **6**, 400–406.

181 J. Bao, X. D. Zhang, B. Fan, J. J. Zhang, M. Zhou, W. L. Yang, X. Hu, H. Wang, B. C. Pan and Y. Xie, *Angew. Chem., Int. Ed.*, 2015, **54**, 7399–7404.

182 Y. Y. Wang, Y. Q. Zhang, Z. J. Liu, C. Xie, S. Feng, D. D. Liu, M. F. Shao and S. Y. Wang, *Angew. Chem., Int. Ed.*, 2017, **56**, 5867–5871.

183 L. Xu, Q. Q. Jiang, Z. H. Xiao, X. Y. Li, J. Huo, S. Y. Wang and L. M. Dai, *Angew. Chem., Int. Ed.*, 2016, **55**, 5277–5281.

184 K. L. Yan, J. Q. Chi, Z. Z. Liu, B. Dong, S. S. Lu, X. Shang, W. K. Gao, Y. M. Chai and C. G. Liu, *Inorg. Chem. Front.*, 2017, **4**, 1783–1790.

185 D. F. Yan, Y. X. Li, J. Huo, R. Chen, L. M. Dai and S. Y. Wang, *Adv. Mater.*, 2017, **29**, 1606459.

186 T. Ling, D. Y. Yan, H. Wang, Y. Jiao, Z. P. Hu, Y. Zheng, L. R. Zheng, J. Mao, H. Liu, X. W. Du, M. Jaroniec and S. Z. Qiao, *Nat. Commun.*, 2017, **8**, 1509.

187 Y. Tong, Y. Q. Guo, P. Z. Chen, H. F. Liu, M. X. Zhang, L. D. Zhang, W. S. Yan, W. S. Chu, C. Z. Wu and Y. Xie, *Chem*, 2017, **3**, 812–821.